Effect of Impulse Noise in Wireless Communications

Report Submitted By

Mohammad Ismail Hossain

Communications, Systems and Electronics

School of Engineering and Science

Jacobs University Bremen

m.hossain@jacobs-university.de

March 21, 2012

Supervisor: Prof. Dr. Werner Henkel

Abstract

In this report, we address the noise which is impulsive, non-Gaussian, and follows a heavy-tailed distribution. In wireless communications, often noise is considered as an additive white Gaussian noise (AWGN). In reality, receivers have omnidirectional capability and it receives many signals which are not only AWGN, it has non Gaussian components. Most commonly used heavy-tailed distributions are Middleton's models (Class A, B, and C), the Symmetric Alpha-Stable distribution, the Gaussian mixture distribution, and the generalized Gaussian distribution. For the detection of signals in the presence of impulsive noise, these models are used to model the effect of impulse noise in wireless receivers. In Middleton's Class-A model, a single antenna system is considered. Recently, McDonald extended this model for two antenna system. In our study, we extended Middleton's Class-A model to make it suitable for multiple-antenna systems. In order to detect and mitigate the effect of impulsive noise, a model for a multiple-antenna system is adopted while this is an accurate model for the thermal noise present at the receiver and measured noise from different noise sources. In addition, an ignition circuit is designed which generates impulse noise similar to the one of car ignition. Measurements are taken from different sources and using measured data, analytical models for the statistics of impulse noise including voltage histograms, probability density functions (pdfs) of voltages, Gaussian-Gaussian model, generalized Gaussian distribution have been developed, where the Gaussian-Gaussian can be seen as for class-A model. The Levenberg–Marquardt algorithm (curve-fitting tool) has been used to demonstrate the approximation of measured data with various model functions. To estimate required parameters, this curve-fitting tool is used, which gives more precise results. Finally, MATLAB simulations have been performed to examine the effects of this non-linearity for both Middleton's Class-A model, Gaussian mixture, and generalized Gaussian distribution.

Contents

Abstract **1**

1 Introduction **5**

2 Background and Methodology **7**
2.1 Impulse Noise 7
2.2 Sources of Impulse Noise 7
2.3 MIMO System 8
2.4 Noise Modeling 8
2.4.1 Middleton's Class-A Model 9
2.4.2 Symmetric Alpha-Stable (SαS) Model 10
2.4.3 Extension of Middleton's Class-A Model for Multi-Antenna System 10
2.4.4 Gaussian Mixture Model 11
2.4.5 Generalized Gaussian Distribution 12

3 Experimental Analysis **13**
3.1 Instrument Set-up for the Measurements 13
3.2 Car Ignition Circuit 14
3.2.1 Switching Circuit 14
3.2.1.1 Relay Driver Circuit 14
3.2.1.2 Voltage-Controlled Oscillator (VCO) 15
3.3 Measurement Techniques 16

4 Simulation Results Based on Measured Data **17**
4.1 Probability Density Function (PDF) Estimation Techniques 17
4.1.1 Method of Moments (MOM) Estimation Technique 17
4.1.2 Measured Data 19
4.1.3 Curve-Fitting Approach 20
4.2 PDF Estimation Using a Curve-Fitting Approach 21
4.2.1 Gaussian-Gaussian Model 24
4.3 Frequency Response for Channels 25

5 Conclusion **26**

Bibliography **27**

List of Figures

3.1 Block diagram of multiple-antenna receiving system 13
3.2 Block diagram of car ignition circuit 14
3.3 Schematic diagram of relay driver. 15

4.1 Impulse segment for inter-antenna distances $3\lambda/4$ from a drilling machine at a distance of 50 cm. 19
4.2 Impulse segment for inter-antenna distances $\lambda/4$ from the car ignition circuit at a distance of 50 cm. 19
4.3 Voltage histograms for inter-antenna distances $\lambda/4$ from the drilling machine at a distance of 50 cm. 20
4.4 Measured probabilty density function. 21
4.5 Impulse noise density with fitted curve. 22
4.6 Gaussian density with fitted-curve. 22
4.7 Overall density and noise contributions. 23
4.8 PDF with fitted-curves for different selected areas and noise contributions. 23
4.9 Gaussian density approximating the outer region. 24
4.10 Overall fitted considered densities. 24
4.11 Frequency responses for (a) Channel 1. (b) Channel 2. 25
4.12 Frequency responses for (a) Channel 3. (b) Channel 4. 25

List of Tables

4.1 Parameters approximation for Gaussian-Gaussian model. 21
4.2 Parameters approximation for the Henkel/Kessler (HK) model. . . . 21
4.3 Mean and variance from different antennas. 22

Chapter 1

Introduction

Wireless technology is the foundation of the much anticipated omnipresent communication networks that allow people and machines to transfer and receive information on the move, anytime, and anywhere. This technology enables an almost endless set of applications such as wireless phones, wireless Internet access, wireless local area networks, smart homes and appliances, automated highways, distance learning, sensor networks, video conferencing, and remote medicine. There are many technical challenges that must be overcome. The most common problem is noise which arises from wireless networks.

In wireless communications systems, various kinds of noise are experienced. In most of the cases, thermal noise is the common one which can be illustrated by a Gaussian model. Nevertheless, wireless communications systems are rarely disturbed by white Gaussian noise, only. Human-made electromagnetic (EM) environments, and many natural ones are fundamentally impulsive and cannot be assumed to be Gaussian. Impulse noise has a highly structured form characterized by significant probabilities of large interference levels and short duration [1]. The impulse noise or electromagnetic interference (EMI) can be found in many indoor and outdoor environments [2]. However, the impulse character can drastically degrade the performance and the reliability of wireless communications systems even in case of high signal to noise ratios (SNRs). In order to guard against unacceptable performance, the true characteristics of the noise must be taken into account. For this reasons, we need to implement appropriate models for impulse noise.

Impulse noise is most frequent in many wireless communication applications. For instance, automotive ignition noise, power transmission lines, corona effect, and arc generating circuit components are examples of impulse noise sources, which are encountered mainly in metropolitan areas [3]. In indoor wireless communications, devices with electromechanical switches such as electrical motors in elevators, refrigerator units, photocopy machines, and printers are considered as impulse noise sources. Furthermore, microwave ovens, drilling machines, trains, trams, cash register receipt printers, gas-powered engines, car ignitions, welding, and compressor motors produce impulse noise in frequency bands which coincide with the operating frequencies of current wireless networks [4, 5]. Due to electromagnetic interference from independent sources, receivers are affected by disruption of radio frequency interference (RFI). There are three sources of impulsive RFI, namely: natural, in-

herent, and man-made. The first case is caused by natural phenomena such as lightning and radiation from the sun and galactic sources. This type of interference is commonly called atmospheric noise. Man-made noise is produced by a number of different classes of electrical and electronic equipment and systems. These sources of impulse noise include high power broadcast systems and a multitude of other communications systems [6].

Impulsive RFI is a combination of independent radiation events prevailing non-Gaussian statistics. Middleton's Class A, B, and C noise models (statistical-physical) and Symmetric Alpha-Stable model (statistical) are used for impulse noise modeling [7, 8]. They are well-suited for modeling the predominantly non-Gaussian random processes that arise from the nonlinear phenomena that govern electromagnetic interference. Symmetric Alpha-Stable processes are included due to their mathematically tractable form for parameter estimators and communication detectors [9]. In this project, we mainly concentrate on Middleton's Class-A model, Gaussian mixture, and a generalized Gaussian distribution (HK model).

In the sense of error-free communication we need to have sufficient knowledge of the sources that might be responsible for causing disturbance in the entire wireless communication systems. So we need to have knowledge of various models commonly used for different noise analysis since different sources produce different kinds of characteristics.

In this project, in order to measure the impulse noise in multiple-input multiple-output (MIMO) wireless systems, we implemented a multi-antenna wireless receiver system that receives the signals in the Wireless LAN frequency range from various sources. With different inter-antenna spacing and distance between source and antenna, we analyzed the effect of impulse noise from different sources. We designed our own ignition circuit that provides an impulse noise environment similar to car ignition inside the lab. Then we tried to model these effects of impulse noise with appropriate model functions and finally, the statistical characteristics of impulse noise were analyzed.

Chapter 2

Background and Methodology

In this chapter, we discuss some necessary theoretical knowledge and methods which are relevant to our study. Essentially, we discuss impulse noise, possible impulse noise sources in wireless environments and multiple-antenna system to measure impulse noise. Furthermore, we discuss the most commonly used heavy-tailed distributions to model this noise.

2.1 Impulse Noise

Impulse noise is an additive disturbance that is only active for very short time intervals. Due to its small duty cycle, the average power of impulse noise is much lower than its instantaneous power during active intervals. This results in a large peak-to-average ratio (PAR) - the salient feature of this type of noise [7]. Impulse noise is a more problematic source of error when it occurs frequently with impulse amplitudes larger than background noise. In this case, the error events are dominated by the impulse noise and its amplitude, duration, and time of occurrence of impulses are random [10]. The inter-arrival time of these impulses is generally assumed to be greater than the time constants of the measuring system. This does not introduce any restrictions, and simply means that individual pulses can be resolved by the system [10].

2.2 Sources of Impulse Noise

There are many potential sources of impulsive noise in the wireless environments. There are mainly three sources of impulsive RFI, which are [4, 6]

1. Natural Source: These type of noise are caused due to natural phenomena such as lightning and radiation from the sun, cosmic, extraterrestrial solar and galactic sources etc.. This type of interference is commonly called atmospheric noise. (Note: The power of non-stationary noise is not a useful quantity one may use the energy and also the energy-density spectrum).

2. Inherent Source: Inherent noise is the noise within electronic equipment.

3. Man-made source: There are many sources of impulse noise which are produced by a number of different classes of electrical and electronic equipment and systems. These sources of impulse noise include high power broadcast systems and a multitude of other communications systems [6]. We can distinguish indoor source and outdoor sources.

   → Indoor sources: In our daily life, we are consecutively using many domestic appliances which produce frequent impulse noise. For example, house appliances such as washing machines, dish washers, refrigerator units, photocopy machines, elevator, food mixers, irons, ovens, kettles, electric razors, drills, central heating thermostats, and light switches are common sources of impulse noise [12].

   → Outdoor sources: In outdoor environments, we may experience various kinds of impulse noise sources, e.g., gas-powered engines, car ignition, welding, compressor motors, high power grid lines, corona effects, and medical equipment are remarkable sources [3].

2.3 MIMO System

In multiple-antenna systems, multiple transmitting and/or multiple receiving antennas are deployed and are often referred to as multiple-input multiple-output (MIMO) or vector systems. Huge gains in data rate for point-to point systems by employing multiple antennas at both the transmitter and receiver. Multiple-input multiple-output (MIMO) techniques are also used to improve the robustness, and performance of wireless links. Here, the term multiple-input multiple-output refers to the use of an array of antennas for both transmitting and receiving [13]. Typically, ground-to-ground links are not line of sight. The electromagnetic waves transmitted from the antennas bounce around the environment in a complicated fashion, and end up at the receiver coming from multiple directions, and with varying delays. The effect produced by the direction/delay interactions is referred to as multipath. In our study, we use an array of monopole antennas only for receiving purpose.

2.4 Noise Modeling

RFI is typically thought of being stationary, e.g., a narrow-band disturber. Two general approaches for modeling electromagnetic interference (EMI) are through physical modeling, and through statistical-physical modeling. In physical modeling, each source of EMI would require a different circuit model. Requires also, statistical-physical model provide universal models for accurately modeling EMI from natural and human-made sources. The key statistical-physical models are the Middleton's Class A, B, and C noise models [7]. Middleton's models are widely accepted, primarily, since these models are canonical, i.e., their mathematical form is independent of the physical environment. Middleton's models are classified with respect to the receiver bandwidth:

Class-A: It is called narrowband noise model, because the interference spectrum is narrower than the receiver bandwidth.

Class-B: This is known as broadband noise model. In this model, the interference spectrum is wider than the receiver bandwidth. The Class-B interference model is analytically more complex since two characteristic functions are needed to approximate the exact characteristic function [7]. Hence, we have two expressions for the envelope density, one for small and intermediate envelope values, and the other for the larger values. The examples of such interference included atmospheric noise, automotive ignition noise, and arc welders.

Class-C: Mixed Case: Since Class-C interference is a sum of the Class-A and Class-B interference models, no specific derivations for Class-C are required. Furthermore, Middleton proved that Class-C can be approximated by Class-B model in most of the cases [7].

Impulse noise models for systems operating at low frequencies have been proposed by the ITU [10]. These models are based on measurements of median levels of interfering noise.

Mathematically, impulsive interference is usually modeled as a train of pulses [11, 12]

$$n(t) = \sum_i A_i P_{w_i}(t - \tau_i). \tag{2.1}$$

where the amplitude A_i and arrival time τ_i of each pulse is a random variable whose distribution is a priori unknown. The shape of the pulses depends especially on the source, also on the measurement frequency range.

Hence, we limit our discussion to the Class-A model, the Gaussian mixture, and the generalized Gaussian distribution for the remainder of the report.

2.4.1 Middleton's Class-A Model

The spectral bandwidth of the noise entering the receiver is comparable to or less than the receiver bandwidth at the receiver's front-end stages. Specifically, Class-A interference produces negligible transients in the typical receiver. This model has been used to develop optimum detection algorithms for a wide range of communications problems [14]. Middleton's Class-A model is the first model which treats narrowband interference processes. An advantage of Middleton's model is that it can be expressed in a canonical form, so that noise from many different specific interference scenarios can all be represented by the same model but with a different set of coefficients. A second important feature of this model is that it is also analytically tractable, as well as computationally manageable [14].

The Class-A probability density function (PDF) can be expressed by

$$P_{class-A} = \sum_{m=0}^{\infty} e^{-A} \frac{A^m}{m!\sqrt{2\pi\sigma_m^2}} e^{-\frac{x^2}{2\sigma_m^2}}, \tag{2.2}$$

where, $\sigma_m^2 = \frac{\frac{m}{A}+\Gamma}{1+\Gamma}$. The Class-A model is uniquely determined by the following two parameters [7]:

→ A is the overlap or impulse index . It is the product of the average number of emissions events impinging on the receiver per second and mean duration of a typical interfering source emission, typically $A \in [10^{-2}, 1]$. The smaller A, the more "structured" (in time) is the interference. Conversely, the larger A, the more Gaussian and less structured is the noise. When A is ∞, the noise is Gaussian [7].

→ Γ is called the Gaussian factor and it is the ratio $\frac{\sigma_G^2}{\sigma_i^2}$, where σ_G^2 is the intensity of the independent Gaussian component, σ_i^2 is the intensity of the impulsive non-Gaussian component, typically $\Gamma \in [10^{-6}, 1]$.

2.4.2 Symmetric Alpha-Stable (SαS) Model

While Middleton's Class-A and Class-B models are known to accurate by model impulse RFI sources, their practical applications are limited due to the intractable form of their distributions [7]. In particular, Class-B interference model is difficult to use due to the existence of six parameters, and also an empirically determined inflection point (ε_B) [3]. Hence many authors have considered the Symmetric Alpha Stable (SαS) model as an approximation to Middleton Class-B model [10]. This approximation is particularly accurate for the case of narrowband reception without a Gaussian component, as well as the case of a symmetric pdf without a Gaussian component.

Symmetric Alpha-Stable (SαS) models are used to model the statistical properties of an "impulse" signal [10]. A random variable is said to have (SαS) distribution if its characteristic function is of the form

$$\phi(\omega) = e^{j\delta\omega - \gamma|\omega|^\alpha}. \tag{2.3}$$

Hence, the following three parameters uniquely identify a (SαS) distribution [10]:

• α is the characteristic exponent and is a measure of the "thickness" of the tail of the distribution, typically $\alpha \in [0, 2]$.

• δ is the localization parameter. It is the mean when $1 \leq \alpha \leq 2$, and the median when $0 \leq \alpha \leq 1$, where$\delta \in [-\infty, \infty]$.

• γ is the scale parameter or the dispersion and is similar to the variance of the Gaussian distribution, where $\gamma \geq 0$.

The Symmetric Alpha-Stable model is ever worse, since it has no closed-form density, only a characteristic function.

2.4.3 Extension of Middleton's Class-A Model for Multi-Antenna System

In Middleton's Class-A model he assumed a single-antenna system for reception. McDonald extended the Class-A model to spatial diversity schemes and defined a multi-dimensional version of Class-A model by developing mathematical expressions for the signals simultaneously received at two antennas after matched filtering. In

order to limit the complexity and to promote clarity, only the two antennas case is considered. The normalized random variable (x, y) PDF for antenna 1 and antenna 2 is [21]:

$$f_R(x,y) = \frac{e^{-A}}{2\pi c_0 c_0' \sqrt{1-k_0^2}} \exp\left(-\frac{\frac{x^2}{c_0^2} + \frac{y^2}{c_0'^2} + \frac{2xyk_0}{c_0 c_0'}}{2(1-k_0^2)}\right) + \frac{(1-e^{-A})}{2\pi c_1 c_1' \sqrt{1-k_1^2}} \exp\left(-\frac{\frac{x^2}{c_1^2} + \frac{y^2}{c_1'^2} + \frac{2xyk_1}{c_1 c_1'}}{2(1-k_1^2)}\right), \tag{2.4}$$

$$\text{where } c_0 = \sqrt{\tfrac{\Gamma_1}{1+\Gamma_1}},\ c_0' = \sqrt{\tfrac{\Gamma_2}{1+\Gamma_2}},\ c_1 = \sqrt{\tfrac{A^{-1}+\Gamma_1}{1+\Gamma_1}},\ c_1' = \sqrt{\tfrac{A^{-1}+\Gamma_2}{1+\Gamma_2}}.$$

A is the so-called overlap index. Γ_1 is the ratio of Gaussian power to the non-Gaussian power for antenna l. Γ_2 is the ratio of Gaussian power to the non-Gaussian power for antenna 2. k_0 is the correlation coefficient of two antennas for the Gaussian component. k_1 is the correlation coefficient of two antennas for the non-Gaussian component [21].

Using this multivariate case, we can modify Middleton's Class-A model for multi-antenna systems. A bivariate Middleton's Class-A model for a 2 antenna system has been considered in [15]. An extension for $n_r \geq 2$ can be expressed as [16]

$$f(x) = \sum_{m=0}^{\infty} a_m g(x, \mu, \sigma_m^2). \tag{2.5}$$

$$\text{where } a_m = \tfrac{e^{-A}A^m}{m!},\ \mu = 0 \text{ and } g(x, \sigma_m^2) = \frac{e^{-\frac{x^2}{2\sigma_m^2}}}{\sqrt{2\pi\sigma_m^2}}.$$

Middleton's Class-A model for multi-antenna system can be represented by [17]

$$f(x) = \sum_{m=0}^{\infty} \frac{\frac{A}{m!}}{(2\pi)^{\frac{n_r}{2}} \left|K_m\right|^{\frac{1}{2}}} e^{-\frac{x^T x K_m^{-1}}{2}}, \tag{2.6}$$

where K_m is an $n_r \times n_r$ covariance matrix and n_r is a number of antennas, and detailed derivation can be found in [17].

2.4.4 Gaussian Mixture Model

A Gaussian Mixture Model is a parametric probability density function represented as a weighted sum of Gaussian component densities, e.g., Middleton's Class-A model. A Gaussian mixture model is commonly used as a parametric model of the probability distribution of continuous measurements. This model can be used as an approximation of a wide variety of symmetric zero-mean random variables, e.g., the Laplace distribution and the SalphaS distribution [6].

The Gaussian-Gaussian model offers an approximation to the Class-A model, The Gaussian-Gaussian model is as follows:

$$P_{class-A} = \frac{e^{-A}}{\sqrt{2\pi\sigma_0^2}} e^{-\frac{x^2}{2\sigma_0^2}} + \frac{1-e^{-A}}{\sqrt{2\pi\sigma_1^2}} e^{-\frac{x^2}{2\sigma_1^2}}, \tag{2.7}$$

where, A is the impulse index, and σ_0, σ_1 are the standard deviations [6].

2.4.5 Generalized Gaussian Distribution

The generalized Gaussian distribution as an impulse noise model was proposed in [6, 18] for modeling the voltage histogram of impulse noise on twisted pairs and resulted from a measurement campaign of Deutsche Telekom, which is called the HK (Henkel/Kessler) model. As an alternative to the symmetric alpha-stable distribution, the generalized Gaussian distribution has been considered for multiple access interference in a direct sequence spread spectrum systems [6].

A suitable approximation can be achieved from [18] for the pure impulse noise density, which can be expressed as

$$f_i\left(u\right) = \frac{e^{-\left|\frac{u}{u_0}\right|^{\frac{1}{5}}}}{10\Gamma\left(5\right)u_0} = \frac{e^{-\left|\frac{u}{u_0}\right|^{\frac{1}{5}}}}{240u_0}\,. \tag{2.8}$$

This is a generalized Gaussian distribution where u is the voltage and u_0 is the reference voltage. Here an offset, of zero is assumed. A non zero offset is, of course realized by replacing u by $(u - u_0)$. This is quite good approximation for pure a impulse noise density. Now, if we include background noise which is the only disturbance between impulses, we obtain the equation in following form,

$$f_{tot}\left(u\right) = Pf_n(u) + (1-P)f_n(u) * f_i(u)\,, \tag{2.9}$$

$$\text{where } f_n\left(u\right) = \tfrac{1}{\sqrt{2\pi\sigma^2}}e^{-\frac{u^2}{2\sigma^2}}.$$

where, $f_n\left(u\right)$ is the Gaussian density of background noise, σ is the standard deviation, and $P \in [0, 1]$ is its relative portion. For $f_{tot}(u)$, during the impulse, background noise is also presentand we can see this represented by a convolution of both densities (Gaussian and Impulse) [18].

Chapter 3

Experimental Analysis

In this chapter, we discuss the total measurement procedures, instrument and devices set up and the overall techniques required for measuring impulse noise from different sources.

3.1 Instrument Set-up for the Measurements

Based on our multiple-antenna system, we installed four antennas resonating at a center-frequency of 2.45 GHz. In order to take measurements, 190 MHz bandwidth filters, 300-4300 MHz mixers, and 1700-4200 MHz power splitter were used. In order to implement the overall set-up, antennas, band-pass filters, down-converting mixers, oscillator, and a digital oscilloscope for acquiring the sampled and down-sampled data at an intermediate frequency were required.

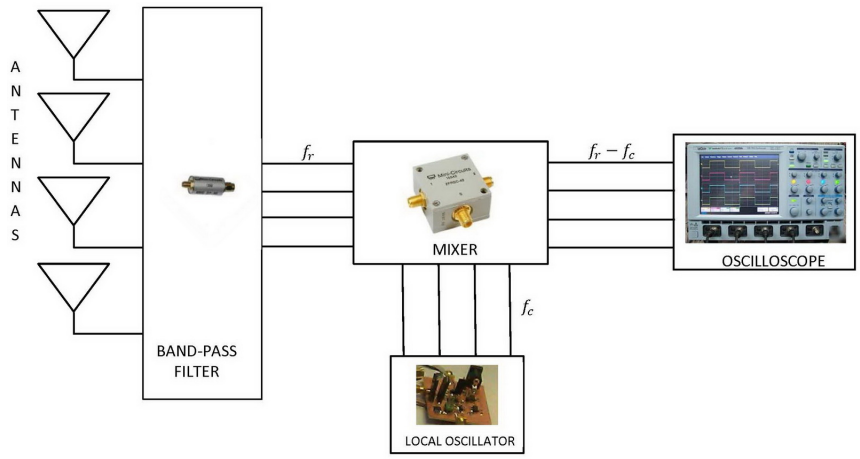

Figure 3.1: Block diagram of multiple-antenna receiving system

In order to take impulse noise measurements, the following steps were taken:

1. Monopole antennas were designed at $\lambda/4$ where λ is the wavelength at 2.45 GHz RF center frequency, and checked for the resonating frequency using the scattering-parameter, i.e., S-parameter S_{11}. These antennas were used only for receiving purposes and they have an omni-directional receiving capability.

The antennas were positioned vertically and equidistant on to a ground plate to form a Uniform Linear Array (ULA).

2. The antennas were connected to band-pass filters with coaxial cables which filtered the RF signal with a bandwidth range from 2530 MHz to 2340 MHz. The outputs of the band-pass filters were linked with mixers which are down-converted according to a local oscillator signal, that was applied to the local-oscillator (LO) input port of the mixer. Signals from both ports are mixed to yield the Intermediate Frequency (IF) of interest. The IF was finally filtered by the oscilloscope itself.

3. All mixers were connected with a power splitter which was provided with the mixing carrier from the local oscillator.

4. In order to supply a 2.1 GHz carrier frequency, a specially programmed signal generator was used.

5. A digital oscilloscope was used for filtering and sampling/storage of the IF signals for further downsampling in a MATLAB routine of a controlling PC.

3.2 Car Ignition Circuit

In the project work, an ignition circuit which provides similar impulse noise like car ignition was designed using a standard ignition coil, spark plug, capacitor, relay driver circuit, relay and a voltage-controlled oscillator (VCO) for rectangular pulses. The frequency of the voltage controlled-oscillator can be chosen by an external capacitor.

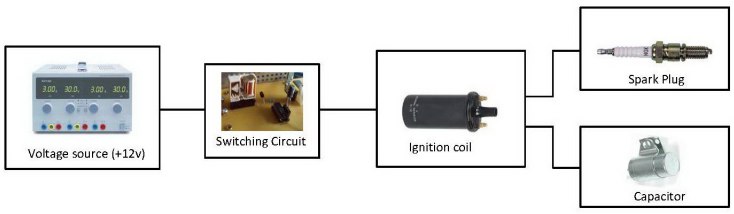

Figure 3.2: Block diagram of car ignition circuit

3.2.1 Switching Circuit

This circuit consists of a relay driver, relay, and voltage-controlled oscillator (VCO). In the following it is described briefly.

3.2.1.1 Relay Driver Circuit

This relay driver circuit switches the current through the relay modulated the breaker contact. A protection diode was used to protect the transistor from the reverse current generated from the coil of the relay during the switch off time. With

refer to figure 3.3, in order to implement relay driver circuit we had to calculate the values of resistor and transistor . The way to calculate them are:

First we calculated the load current:

$$I_L = \frac{V_S}{R_L}\,, \tag{3.1}$$

Then we calculated the transistor h_{FE}. It is needed to be at least 5 times the load current I_L divided by the maximum output current from the input to the base of the transistor.

$$h_{FE}\,(min) > 5 \times \frac{I_L}{I_{input}}\,, \tag{3.2}$$

Now the transistor Q_s according to its current gain h_{FE} has been selected. Then the calculated the base resistor R_B was in the form

$$R_B = 0.2 \times R_L \times h_{FE}\,. \tag{3.3}$$

Figure 3.3 shows the schematic diagram of our relay driver where we used our calculated base resistor and transistor to acquire expected current through relay.

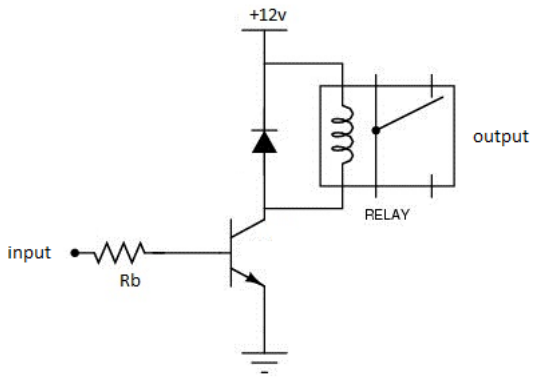

Figure 3.3: Schematic diagram of relay driver.

The considered protective diode was 1N4001 suit can be any which is used to protect the transistor from reverse current generated from relay.

3.2.1.2 Voltage-Controlled Oscillator (VCO)

A voltage controlled oscillator is used as a rectangular pulses generator. It has a typical maximum frequency of 85 MHz, frequency spectrum range 1 Hz to 60 MHz and a power dissipation of 525 mW. The output frequency of the oscillator can be controlled by changing an external capacitor and approximated as follows:

$$f_0 = (\frac{5 \times 10^{-4}}{C_{ext}})\,, \tag{3.4}$$

where the frequency is in Hz and the capacitance is in Farad.

The following are the components to implement this circuit:

1. Voltage-Controlled Oscillator (exact value similar to SN54S124).

2. Resistor (3.7k).
3. Diode (1N4001).
4. NPN Transistor (2N2219A).
5. Relay Coil (172 Ohms).
6. Capacitors (2.2 μF, 4.7 μF, 10 μF, 20 μF, 100 μF).
7. Ignition Coil.
8. Spark plug .
9. Capacitor for ignition coil (22 μF standard).
10. Voltage source.
11. Voltage regulator (7805): for converting voltage from 12 V to 5 V.

3.3 Measurement Techniques

Impulse noise generates from different sources such as drilling machine, car ignition circuit were analyzed. In order to take appropriate measurements the antennas were placed at suitable places, and inter-antenna distances. All coaxial cable connections had to be constructed. By using a Vector Network Analyzer (VNA), connection cables and transfer function of the filter-mixer pairs were measured for calibrating purposes.

Using data-acquiring Matlab code, impulse segments were taken from different sources through the digital oscilloscope. In order to take measurement, we have considered millions of sample to get accurate result. The signal was sampled at 5 GHz, and saved after down-sampling with 2.5 GHz and the segment time of impulse was 0.2 μs. The measurements were taken at distances of 50 cm and 100 cm from both drilling machine and the car ignition circuit. The inter-antenna distances were considered of $\lambda/4$ and $3\lambda/4$.

During measurements with the car ignition circuit, inside the relay and the spark plug, sparks were observed. Correspondingly, the oscilloscope was triggered and noise segments were stored and counted.

Chapter 4

Simulation Results Based on Measured Data

In this chapter, we discuss parameter estimation algorithms and techniques for various noise models as described earlier. After that, we discuss approximation methods to estimate the parameters.

4.1 Probability Density Function (PDF) Estimation Techniques

There are several algorithms and techniques for parameter estimation, e.g., gradient methods, simplex (Nelder-Mead) method, differential evaluation method, least squares method, method of moments, Newton-Gauss method, Levenberg-Marquart method and other graphical methods [19]. It is difficult to apply these methods on measured data without having knowledge about the pdf. In the following subsections, we will discuss one method of parameter estimation technique and our proposed approach which is based on a curve-fitting tool.

4.1.1 Method of Moments (MOM) Estimation Technique

The method of moments is a technique for parameter estimation, that is based on matching the sample moments to the corresponding distribution moments. The method of moments is the oldest method of deriving point estimators. The method of moments offers a straight forward strategy for devising estimators that have seen proven to be consistent under very general assumptions. The method of moments may also lead to multiple estimators [19]. In such cases, we turn to the generalized method of moments as a single consistent estimator. The method of moments technique can be applied to the generalized Gaussian distribution, Middleton's models, and the Gaussian mixtures model, hence, MOM is described below for Middleton's Class-A model [20].

From equations (2.2) and (2.3), an appropriate probability density function (PDF) is acquired. Since the Gaussian-Gaussian model offers a possible approximation to the Class-A model, a parameter estimation is close used for this model.

The Gaussian-Gaussian model is as follows:

$$P_{class-A} = \frac{e^{-A}}{\sqrt{2\pi\sigma_0^2}} e^{-\frac{x^2}{2\sigma_0^2}} + \frac{1-e^{-A}}{\sqrt{2\pi\sigma_1^2}} e^{-\frac{x^2}{2\sigma_1^2}}. \tag{4.1}$$

Parameters to be estimated are A, σ_0, and σ_1. The estimation procedure can be performed in two ways, one is based on the method of moments [19, 20], and another is using our approximation routine.

the estimation procedure based on the method of moments (MOM): Let, a, b, and c denote for the following moments computed based on the received signal v.

$$a = \sqrt{\frac{\pi}{2}} E\{|v|\} = e^{-A}\sigma_0 + (1-e^{-A})\sigma_1\,, \tag{4.2}$$

$$b = E\{v^2\} = e^{-A}\sigma_0^2 + (1-e^{-A})\sigma_1^2\,, \tag{4.3}$$

$$c = \sqrt{\frac{2\pi}{4}} E\{|v|^3\} = e^{-A}\sigma_0^3 + (1-e^{-A})\sigma_1^3, \tag{4.4}$$

from which, we can find the standard deviations [20]:

$$\sigma_0 = \frac{ab - c + \sqrt{(ab-c)^2 - 4(a^2-b)(b^2-ac)}}{2(a^2-b)}\,, \tag{4.5}$$

$$\sigma_1 = \frac{ab - c - \sqrt{(ab-c)^2 - 4(a^2-b)(b^2-ac)}}{2(a^2-b)}\,. \tag{4.6}$$

Actually, a, b, and c can simply be obtained from the empirical moments over $1 \times N_s$ (length of data vectors) observations:

$$a = \sqrt{\frac{2}{\pi}} \left(\frac{1}{N_s} \sum_{k=1}^{N_s} |v_k| \right), \tag{4.7}$$

$$b = \frac{1}{N_s} \sum_{k=1}^{N_s} v_k^2\,, \tag{4.8}$$

$$c = \sqrt{\frac{4}{2\pi}} \left(\frac{1}{N_s} \sum_{k=1}^{N_s} |v_k|^3 \right), \tag{4.9}$$

where, N_s is the number of sample points. The final weighting constant A can be obtained as

$$A = -\ln\left(1 - \frac{\sigma_0 - a}{\sigma_0 - \sigma_1}\right). \tag{4.10}$$

4.1.2 Measured Data

We visualized the saved data with different approaches. Figure 4.1 shows time segments of different antenna channels from a drilling machine. If we observe these plots below, we can see slight differences between different channels. Figure 4.2 shows data from car ignition.

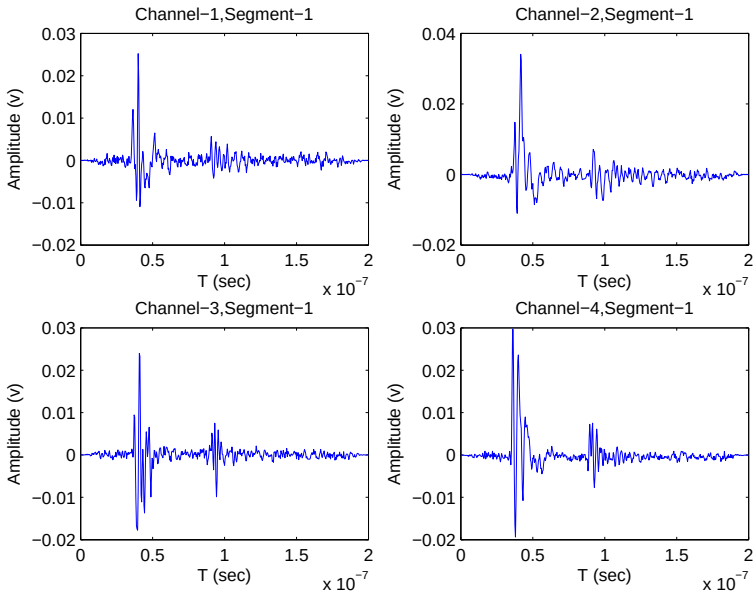

Figure 4.1: Impulse segment for inter-antenna distances $3\lambda/4$ from a drilling machine at a distance of 50 cm.

From figure 4.1 some changes are observed between channels with amplitudes, and different segments are aquired from drilling machine.

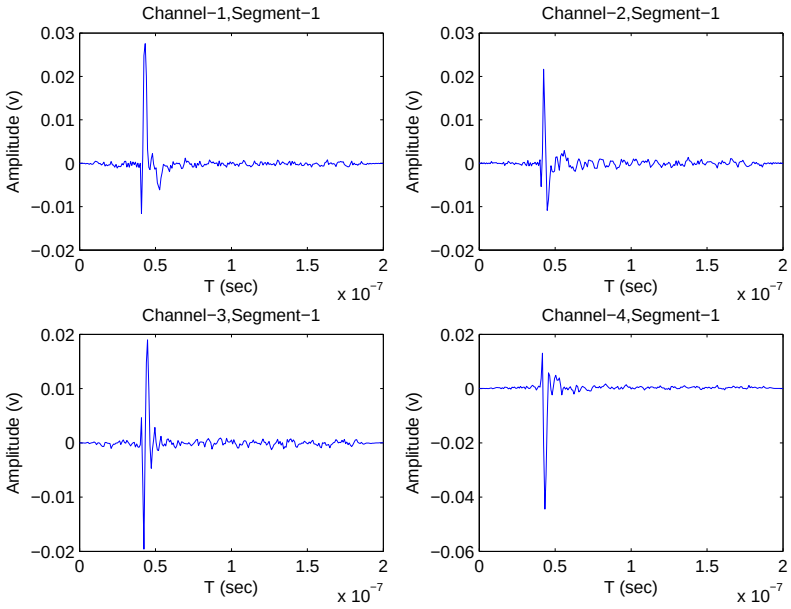

Figure 4.2: Impulse segment for inter-antenna distances $\lambda/4$ from the car ignition circuit at a distance of 50 cm.

From the above figure 4.2, we can observe some changes between channels with amplitudes, and different segments are aquired from car ignition. Comparing the impulse segments of the car igntion to the drilling machine, we can clearly observe that we get weak impulse segments for the car ignition than that of the drilling machine.

Based on our measured data, voltage histograms for different channels are achieved. Figure 4.3 shows these histograms.

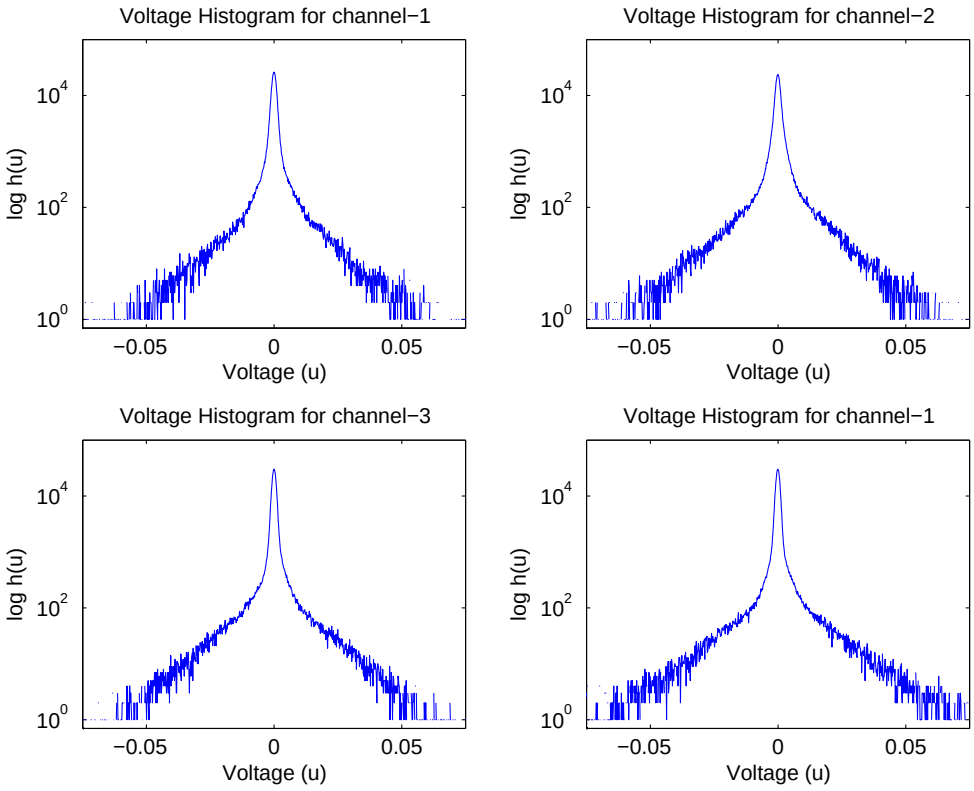

Figure 4.3: Voltage histograms for inter-antenna distances $\lambda/4$ from the drilling machine at a distance of 50 cm.

From figure 4.3, we can notice subtle differences among the four histograms. We have also measured data from drilling machine for inter-antenna distances $3\lambda/4$ from the drilling machine at a distance of 50 cm, 100 cm, and 150 cm.

4.1.3 Curve-Fitting Approach

As we described earlier, we focused on the curve-fitting approach. Here to, based on our measured data, we apply a curve fitting approach to approximate the measured probability density function. The pdf of the measured data can be seen in figure 4.4 In this figure, we can see that the inner area close to zero is most likely Gaussian and the outer area seems to follow a heavy-tailed distribution. Hence, Gaussian model is considered for inner area and heavy-tailed distribution model is considered for outer area on our measured pdf for the curve-fitting purpose.

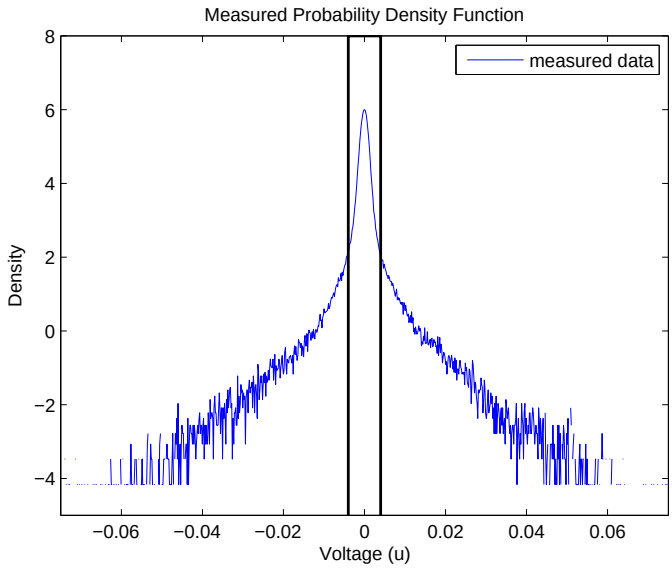

Figure 4.4: Measured probabilty density function.

From Eq. (2.8), the parameters to be determined are A, σ_0, and σ_1. In Table 4.1, we provide the values of the estimated parameters.

Table 4.1: Parameters approximation for Gaussian-Gaussian model.

Parameters	A	σ_0 (mV)	σ_1 (mV)
Values	0.04	0.912	20.63

From Eq. (2.9), an appropriate approximation for pure impulse noise density is achieved. Using equations (2.9) and (2.10), we were estimating the unknown parameters. From our measured data, voltage histograms and probability density functions were plotted. Then, we tried to fit curves for the outer area with pure impulse noise, and the middle part for the Gaussian contribution. From the outer area, we estimated u_0 and from the inner part we estimated σ. Finally, we estimated P for the overall distribution, which is a mix of impulse and background noise. Our approximation tool allows to arbitrarily choose areas to concentrate on dedicated components. Table 4.2 summarizes to obtained parameters.

Table 4.2: Parameters approximation for the Henkel/Kessler (HK) model.

Parameters	P	σ (mV)	u_0 (nV)
Values	0.06594	0.891	81.395

4.2 PDF Estimation Using a Curve-Fitting Approach

We estimated the mean (μ) and variance (σ^2) of the background noise of every antenna channel which are documented in Table 4.3.

Table 4.3: Mean and variance from different antennas.

Channel	mean (μ) in V	variance (σ^2) in V
Channel 1	-1.5277×10^{-19}	1.3042×10^{-5}
Channel 2	1.7941×10^{-19}	1.8582×10^{-5}
Channel 3	3.9080×10^{-20}	1.6223×10^{-5}
Channel 4	-2.6645×10^{-19}	2.1257×10^{-5}

Figure 4.5 shows the estimated approximation for the pure impulse noise density together with the measured frequency distribution and we computed the approximation for the outer areas.

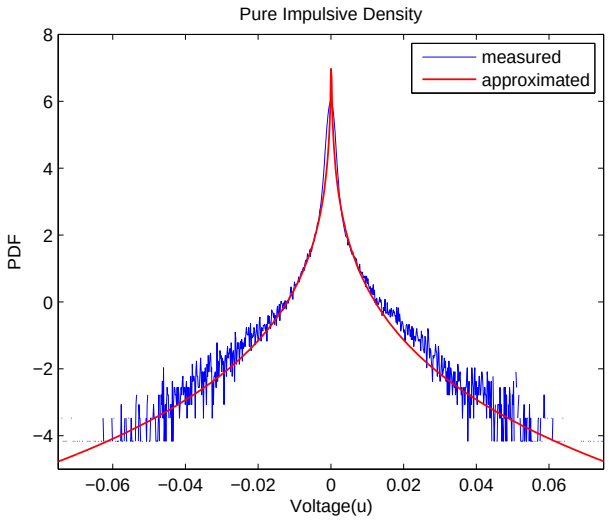

Figure 4.5: Impulse noise density with fitted curve.

Figure 4.6 shows the estimated approximation with the Gaussian noise density with measured density in the inner area.

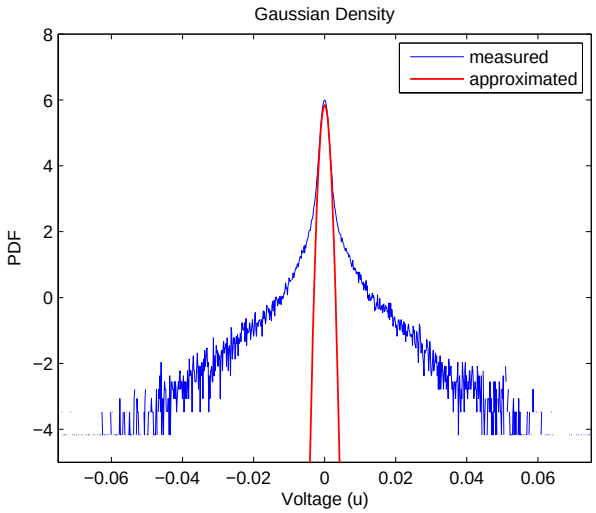

Figure 4.6: Gaussian density with fitted-curve.

From our measured pdf we observe that both Gaussian component and impulse component are present. From the HK model for overall density, we can see the effect of background noise which is convolved with impulse density. After convolving both, the pure impulse density and the Gaussian density, we can see the overall effect in Figure 4.7. From this approximation we obtain the value of P which is between 0 and 1.

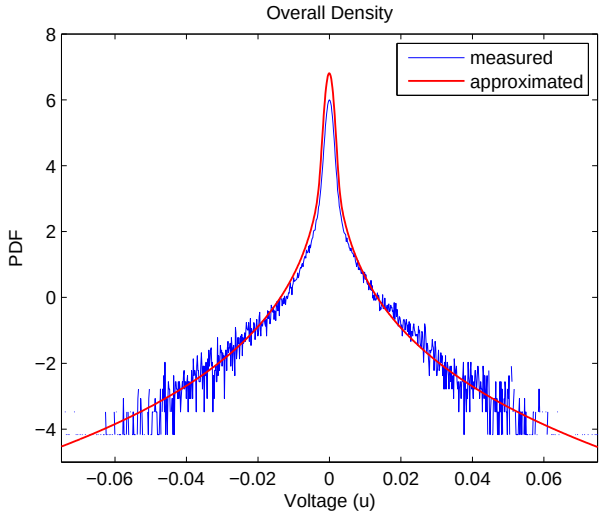

Figure 4.7: Overall density and noise contributions.

Figure 4.8 shows plots for the different selected areas and noise contributions.

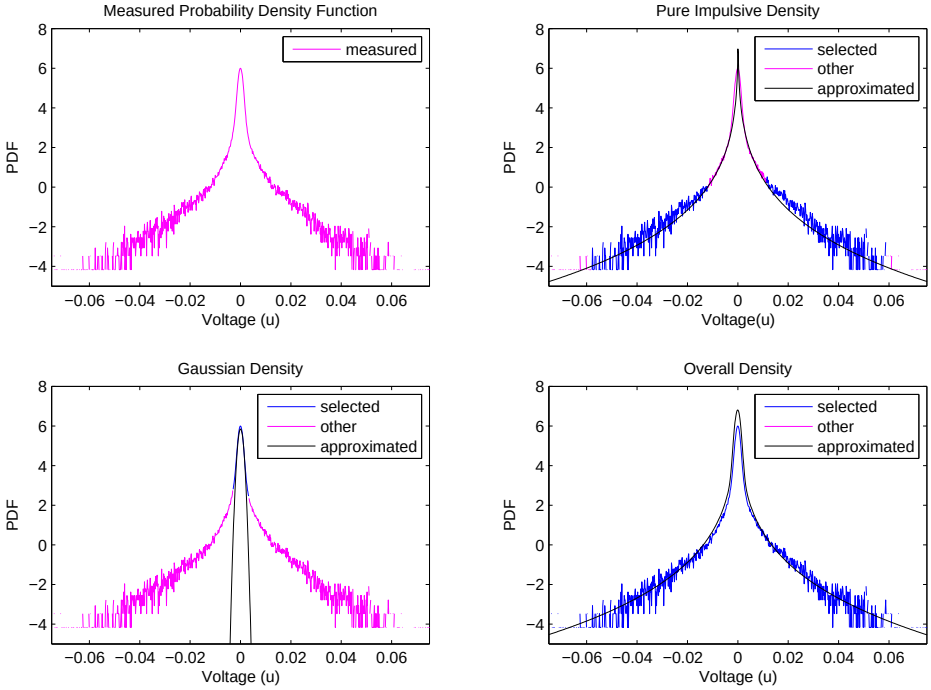

Figure 4.8: PDF with fitted-curves for different selected areas and noise contributions.

4.2.1 Gaussian-Gaussian Model

We also applied this approximation method for the Gaussian-Gaussian distribution and it is nicely fitted with our measured pdf. From this approximation routine we can obtain required parameters and also for manually selected areas to see the noise contributions which lead to figure 4.9 and 4.10.

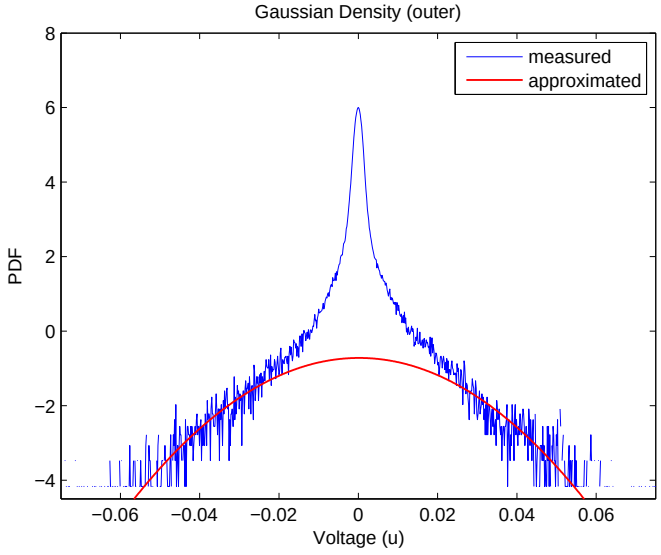

Figure 4.9: Gaussian density approximating the outer region.

Figure 4.9 shows the estimated approximation with the Gaussian noise density with measured density in the outer area and Figure 4.10 shows the estimated approximation with the Gaussian noise density with measured density for the overall region.

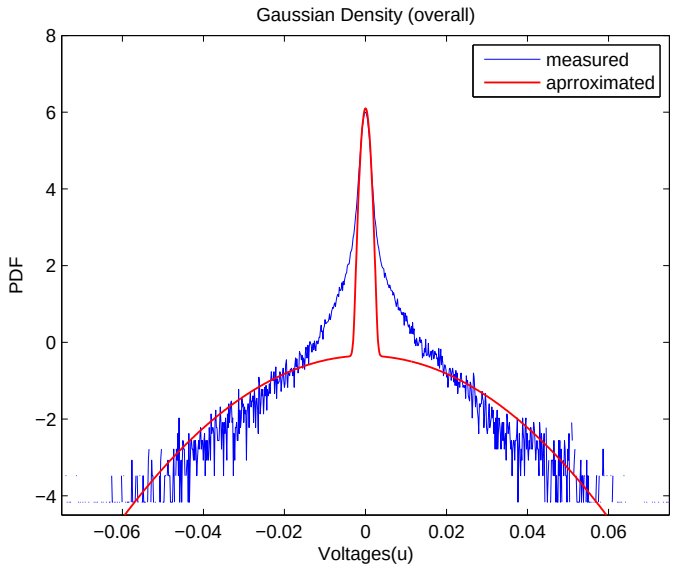

Figure 4.10: Overall fitted considered densities.

4.3 Frequency Response for Channels

We calibrated the channels with filters, mixers, carrier generator, and coaxial cables by measuring the transfer functions. The frequency responses for the different channels are depicted in the following figures. We measured the magnitudes and phases simultaneously with the help of a Vector Network Analyzer.

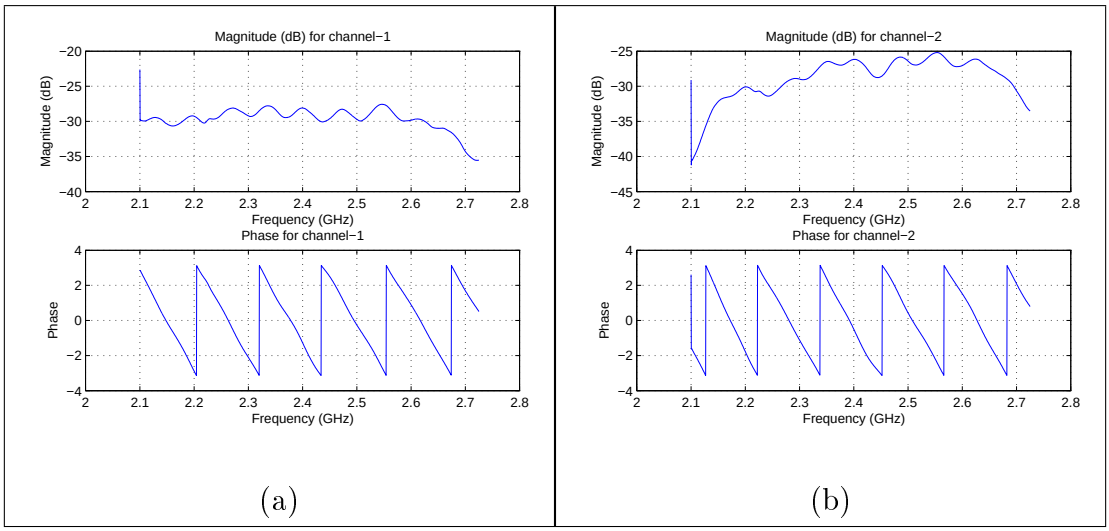

Figure 4.11: Frequency responses for (a) Channel 1. (b) Channel 2.

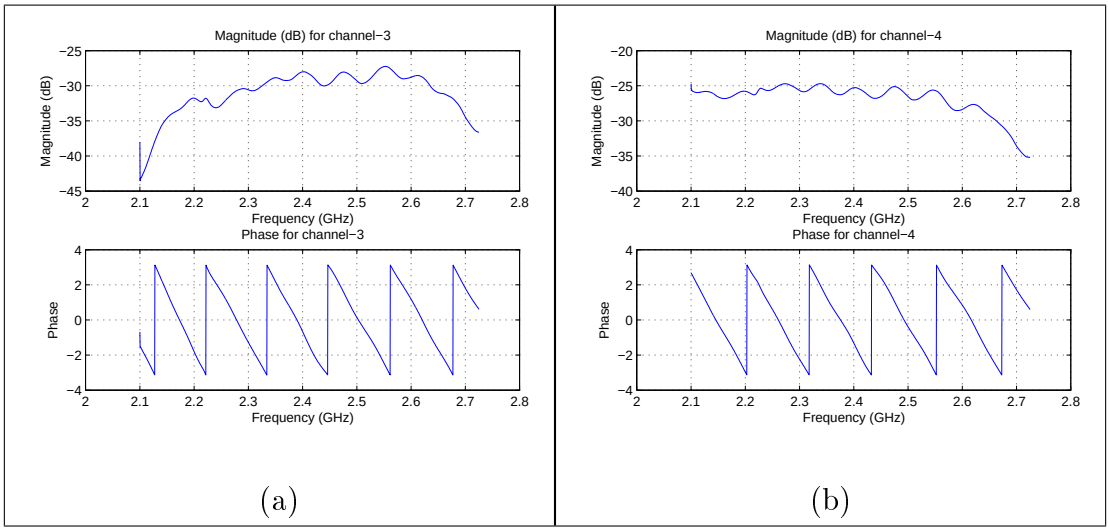

Figure 4.12: Frequency responses for (a) Channel 3. (b) Channel 4.

Using the frequency responses, we are able to normalize our measurement data for each channel.

Chapter 5

Conclusion

In our project, we mainly handled the generation of impulse noise, its detection, reception, and analysis. We discussed different types of impulsive RFI noise sources. We have shown the effect of impulse noise on a multi-antenna system and have seen the different characteristics of indoor and outdoor noise sources. We designed a car ignition circuit for generating such noise inside the lab. Then, we provided a mathematical description of the noise statistics, i.e., various models are proposed. After that, this report provided various algorithms that can be used to estimate the parameters of the mentioned models. We approximated our measured histograms with various model functions, e.g., Gaussian-Gaussian model, the HK model for a pure impulse density and for an impulse density with background noise. We applied an approximation routine based on the Levenberg–Marquardt algorithm to estimate parameters and this approximation routine can be used for various scenarios.

Acknowledgement

I would like to express my heartiest gratitude to Professor Dr. Werner Henkel for his kind and scholastic supervision with stimulating suggestions and encouragement to accomplish this project. I would also like to thank Khodr Saaifan for his kind support during this work.

Bibliography

[1] A. Spaulding and D.Middleton, "Optimum Reception in asn Impulsive Interference Environment-part 1: Coherent Detection," *IEEE Transactions on Communications*, no. 9, pp. 910–923, sept. 1977.

[2] J. D. Parsons, "The Mobile Radio Propagation Channel," *New York: Wiley*, 1996.

[3] E. N. Skomal, "The Range and Frequency Dependence of VHF-UHF Man-made Radio Noise in and above Metropolitan Areas," *IEEE Trans. on Veh. Technol.*, vol. 19, no. 2, pp. 213-221, May 1970.

[4] K. L. Blackard, T. S. Rappaport, and C. W. Bostian, "Measurements and Models of Radio Frequency Impulsive Noise for Indoor Wireless Communications," *IEEE J. Select. Areas in Commun.*, vol. 11, no. 7, pp. 991-1001, Sept. 1993.

[5] M. S. Kuran and T. Tugcu, "A Survey on Emerging Broadband Wireless Access Technologies," *Computer Networks*, vol. 51, no. 11, pp. 3013-3046, Jan. 2007.

[6] Khodr Ahmad Saaifan, "Signal Detection in Non-Gaussian Interference for Wireless MIMO Systems," *Ph.D Proposal.*

[7] D. Middleton, "Non-Gaussian Noise Models in Signal Processing for Telecommunications: New Methods and Results for Class A and Class B Noise Models," *IEEE Trans. on Info. Theory*, vol. 45, no. 4, pp. 1129–1149, 1999.

[8] J. G. Gonzalez and G. R. Arce, "Optimality of the Myriad Filter in Practical Impulsive-Noise Enviroments," *IEEE Trans. on Signal Processing*, vol. 49, no. 2, pp. 438–441, February 2001.

[9] S. M. Zabin and H. V. Poor, "Efficient Estimation of Class A Noise Parameters via the EM [Expectation-Maximization] Algorithms," *IEEE Trans. on Info. Theory*, vol. 37, no. 1, pp. 60–72, January 1991.

[10] A. Shukla, "Radio Communications Agency – Feasibility Study into the Measurement of Man-made Noise," *DERA/KIS/COM/CR10470*, March 2001.

[11] M.C. Jeruchim, P. Balaban and K.S. Shanmugan, "Simulation of Communication Systems: Modelling, Methodology and Techniques," *2nd Ed. Kluwer Academic, Plenum Publishers*, August 2000.

[12] K.L. Blackard, T.S. Rappaport and C.W. Bostian, "Measurements and Models of Radio Frequency Impulsive Noise for Indoor Wireless Communications," *IEEE Journal on Selected Areas in Comms.,* Vol. 11, No. 7, September 1993.

[13] D.W. Bliss, K.W. Forsythe, and A.M. Chan, "MIMO Wireless Communication," *Lincoln Laboratory Journal*, vol. 15, no. 1, pp. 97–126, 2005.

[14] D. Middleton, "Canonical Non-Gaussian Noise Models: Their Implications for Measurement and for Prediction of Receiver Performance," *IEEE Transactions on Electromagnetic Compatibilty*, Vol. EMC-21, No. 3, August 1979.

[15] K. Gulati, A. Chopra, R. Heath, B. Evans, K. Tinsley, and X. Lin, "MIMO Receiver Design in the Presence of Radio Frequency Interference," *IEEE Global Communications Conference*, 2008.

[16] Ghadir Madi, Baptiste Vrigneau,Yannis Pousset, Rodolphe Vauzelle, and Basile L. Agba, "Impulsive Noise of Partial Discharge and its Impact on Minimum Distance-Based Precoder of MIMO system," *18th Eu- ropean Signal Processing Conference (EUSIPCO-2010), Aalborg, Den- mark,* August 23-27, 2010.

[17] P. A. Delaney, "Signal Detection in Multivariate Class-A Interference," *IEEE Transactions on Communications*, vol. 43, no. 4, pp. 365-373, April 1995.

[18] W. Henkel and T. Kessler, "A Wideband Impulsive Noise Survey in the German Telephone Network Statistical Description and Modeling," *AEU*, vol. 48, no. 1, pp. 277–288, November 1994.

[19] K. Fukunaga and T. E. Flick, "Estimation of the Parameters of a Gaussian Mixture using the Method of Moments," *IEEE Trans. Pattern Anal. Mach. Intell.,* vol. PAMI-5, pp. 410–416, Jul. 1983.

[20] J. Agard, "Mélange de deux populations normales et études de quelques functions f(x; y) de variables normales x; y," *Revue de statistique appliquée,* pp. 53–70, 1961.

[21] K. F. McDonald and R. Blum, "A Statistical and Physical Mechanisms-Based Interference and Noise Model for Array Observations," *IEEE Transactions on Signal Processing,* vol. 48, No. 7, pp. 2044-2056, July. 2000.